약학석사 학위논문

새로운 히스톤 탈아세틸화효소 6 억제제인 CKD-M808이 류마티스 관절염 환자의 활막세포와 조절 T 세포에 미치는 영향

Effects of CKD-M808, a novel histone deacetylase 6 inhibitor, on fibroblast-like synoviocytes and regulatory T cells in rheumatoid arthritis

2018년 2월

서울대학교 융합과학기술대학원

분자의학 및 바이오제약학과

손 세 희

Abstract

Effects of CKD-M808, a novel histone deacetylase 6 inhibitor, on fibroblast-like synoviocytes and regulatory T cells in rheumatoid arthritis

SEHUI SHON

Department of Molecular Medicine and

Biopharmaceutical Sciences

The Graduate School

Seoul National University

Background: Rheumatoid arthritis (RA) is a chronic autoimmune inflammatory disease whose hallmark is joint destruction caused by synovial proliferation and leukocyte infiltration in synovial membrane. Histone deacetylase (HDAC) inhibitor was suggested as a promising therapeutic agent in cancer and autoimmune diseases. Recently, the toxicity of pan-HDAC inhibitor (pan-HDACi) has been reported in clinical trials. HDAC6 is a member of HDAC family, mainly targeting non-histone proteins. We examined the therapeutic effect of selective inhibitor of HDAC6 in RA.

Objective: We investigated anti-inflammatory effects of a novel HDAC6 inhibitor, CKD-M808 (M808), on fibroblast-like

synoviocytes (FLS), peripheral blood mononuclear cells (PBMCs) and regulatory T cells (Treg) in RA as well as adjuvant-induced arthritis (AIA) rat model.

Methods: Cell viability was analyzed by cell-counting kit 8 (CCK-8). RA FLS were incubated with HDAC6 inhibitor, M808 and tubastatin A as a positive control, and then stimulated with IL-1β. The levels of metalloproteinase (MMP) -1, MMP-3, IL-6, CCL2, CXCL8, and CXCL10 were measured in culture supernatants of FLS by Magnetic Luminex Screening Assay multiplex kit (Luminex assay) or enzyme-linked immunosorbent assay (ELISA). Expression of HDAC6, α-tubulin, acetylated tubulin, cortactin, acetylated cortactin, ICAM-1, VCAM-1, and GAPDH in FLS were assessed by western blot. Wound healing assay and cell adhesion assay in FLS were performed. RA PBMCs were incubated with HDAC6 inhibitors, tubastatin A or M808, and then stimulated with LPS. TNF-α, IL-1β, IL-6, and IL-10 were measured in culture supernatants of PBMCs by Luminex assay and ELISA. CD4+CD25- T cells were isolated from RA PBMCs and induced to regulatory T cells. The markers of induced Treg (iTreg) were analyzed by flow cytometry. CD4+CD25- T cells (effector T cells, Teff) from healthy donor or murine splenocytes were stained with carboxyfluorescein succinimidyl ester (CFSE) or eFluor®670 and cocultured with iTreg from RA patients or Treg from murine splenocytes respectively. The proliferation of healthy Teff was

analyzed by flow cytometry. Adjuvant-induced arthritis (AIA) was developed in Lewis rat. Clinical score of arthritis was measured after M808 treatment.

Result: M808 decreased the production of MMP-1, MMP-3, IL-6, CCL2, CXCL8, and CXCL10 in RA FLS. M808 increased the acetylation of tubulin and cortactin and inhibited the expression of ICAM-1 and VCAM-1 in RA FLS. The migration of RA FLS and adhesion of U937 cells or Jurkat cells on RA FLS were declined with the treatment of M808. M808 reduced TNF-α and increased IL-10 production, but had negligible effects on IL-1β and IL-6 in RA PBMCs. The function of iTreg induced from RA cells under the presence of M808 significantly improved by suppressing the proliferation of Teff. M808 had enhanced suppressive function of Treg and improves the clinical score of arthritis in AIA rat model.

Conclusion: A novel HDAC6 inhibitor, M808 exhibits the suppressive effects on inflammation by reducing the production of MMPs, pro-inflammatory cytokines, and chemokines, decreasing cell migration and adhesion of RA FLS, and improving the suppressive function of Treg derived from RA patients. M808 improved clinical score of arthritis in AIA animal model. M808 could be a potential therapeutic agent in RA.

Key words: histone deacetylase 6, histone deacetylase inhibitor,

rheumatoid arthritis, inflammation, fibroblast-like synoviocytes, regulatory T cells, cell migration

Student number: 2015-26078

Contents

List of tables

List of figures

Introduction

Post-translational modifications of histone including phosphorylation, methylation, and acetylation regulate gene expression by remodeling of chromatin structure. The acetylation of histone is probably the most studied modification among them. Histone acetyltransferases (HATs) and histone deacetylases (HDACs) are the key enzymes involving this process. HDACs remove the acetyl groups on ε-amino groups of lysine residues of nuclear histone proteins tail, inducing tight DNA packaging which causes transcriptional repression. HATs carry out the opposite action of HDACs, causing transcriptional activation. HATs and HDACs can affect non-histone proteins as well [1, 2].

Mammalian HDACs consist of 18 members in 4 classes including nuclear class I (HDAC1, 2, 3, 8), class IIa (HDAC4, 5, 7, 9), class IIb (HDAC6, 10), NAD-dependent sirtuin (Sirt) class III (Sirt1, 2, 3, 4, 5, 6, 7), and class IV (HDAC11). Class II HDACs are able to shuttle in and out of the nucleus due to the existence of both nuclear localization signal (NLS) and nuclear export signal (NES) [1].

Among HDAC family, HDAC6 belongs to class IIb and it is mainly located in cytoplasm. HDAC6 exclusively possesses two active catalytic domains and targets non-histone proteins such as α-tubulin, cortactin, heat shock protein (Hsp) 90, and Tat rather than histones. Through the interaction with its partners, HDAC6

participates in a variety of cellular processes including cell migration, cell-to-cell interaction, immune response, cell proliferation, degradation of misfolded proteins, and stress response. Recent studies reported that HDAC6 is involved in the pathogenesis of cancer, neurological disorders, and inflammatory disease by interacting with its partners [3-6].

Rheumatoid arthritis (RA) is a chronic autoimmune inflammatory disease characterized by synovial inflammation and proliferation with joint destruction and damage. Synovitis arises from the activation, recruitment, and infiltration of mononuclear cells including T lymphocytes, B lymphocytes, dendritic cells, and macrophages to synovial membrane at the local site of joint. CD4+ T cells primarily contribute to activate monocytes, macrophages, and fibroblast-like synoviocytes (FLS) by activating themselves through cell-to-cell contact or cytokines such as tumor necrosis factor (TNF)-α and interleukin (IL)-17. Activated monocytes, macrophages, and FLS secrete pro-inflammatory cytokines including TNF-α, IL-1, and IL-6, which is the pivotal for chronic inflammation. Not only cytokines, but also chemokines, metalloproteinases (MMPs), angiogenesis factors, adhesion molecules, and cell surface molecules such as co-stimulatory molecules are associated with pathogenesis of RA [7].

It was reported that HDAC activity is upregulated in synovial tissues of RA patients [8] and the modulation in HDAC expression and activity affects peripheral blood mononuclear cells (PBMCs)

and FLS of RA patients [9]. In addition, some studies have shown the benefits of HDAC inhibition by reporting that pan-HDAC inhibitor (HDACi) prevents bone destruction in RA [10], modulates the differentiation, proliferation, and inflammation of leukocytes [11], and suppresses IL-6 production in RA FLS and macrophage [12]. The treatment of pan-HDACi, however, showed undesirable side effects such as fatigue, diarrhea, nausea, and thrombocytopenia, suggesting that a specific inhibition of HDAC is needed [13]. Some previous studies have found that HDAC6-deficient mice survive without any abnormal development or defects in major organs [14] and a selective HDAC6 inhibitor, tubastatin A, showed anti-rheumatic effects in THP-1 cells, Raw 264.7 cells, and collagen induced arthritis (CIA) mouse model [15], indicating that HDAC6-specific inhibition can be considered for the alternative clinical application to pan-HDACi with fewer side effects. In addition, CKD-L, one of HDAC6 inhibitors, decreased arthritis score in CIA mouse model in our previous study [16].

In this study, we investigated the potential influence of a novel HDAC6i, CKD-M808 (M808), in comparison with tubastatin A by evaluating its effects on the production of cytokines, chemokines, cell migration, and adhesion in FLS, the function of regulatory T cells (Treg) from PBMCs in RA or mouse splenocytes, and clinical score of arthritis in adjuvant-induced arthritis (AIA) model.

Methods

Drugs and chemicals

CKD-M808 (M808) and tubastatin A were provided from Chong Kun Dang Pharmaceutical Corporation (CKD Pharm). These chemical were dissolved in dimethyl sulfoxide (DMSO, Sigma-Aldrich, MO, USA) and stored at -20℃.

Enzyme assay

HDAC enzyme panel assay was performed by Reaction Biology Corp. (PA, USA) according to their validated protocol.

Patient samples and cell preparation

Patient samples

All enrolled patients fulfilled the 1987 American College of Rheumatology (ACR) criteria for the classification of RA [17].

FLS were obtained from synovial tissues of RA patients. After chopping synovial tissues with sterile surgical blade and forceps, the specimens were incubated at 37℃ in serum free DMEM (Welgene, Gyeongsangbuk-do, Republic of Korea) with 1 mg/ml type II collagenase (Worthington, OH, USA). Incubated tissues were washed with phosphate buffered saline (PBS) and filtered using 40 μm cell strainer. Filtered cells were cultured in DMEM containing 10% (V/V) fetal bovine serum (FBS, Gibco,

ThermoFisher Scientific, MA, USA) and 1% penicillin/streptomycin (P/S, Gibco). We used FLS between passage 4 and 8 in experiments. Prepared FLS were pretreated vehicle (DMSO) or HDAC6 inhibitor (M808 or tubastatin A) in DMEM containing 1% FBS and 1% P/S for 1 hour and stimulated with interleukin (IL)-1β (R&D systems, MN, USA) 10 ng/ml for 24 hours or 72 hours.

PBMCs were isolated from heparinized blood of RA patients using Ficoll-Paque PLUS solution (GE Healthcare Bio-Science, Uppsala, Sweden). Isolated PBMCs were preincubated with vehicle or HDAC6 inhibitors in RPMI 1640 (RPMI, Welgene) containing 1% FBS and 1% P/S for 1 hour prior to stimulation with lipopolysaccharide (LPS, Sigma-Aldrich) 100 ng/ml for 24 hours. The concentration of HDAC6i was at the range from 0.1 to 5 μM in experiments. Specimens were collected under the Institutional Review Board-approved protocol and informed consent was obtained from each donor.

Cell lines

U937 cells, a human monocyte cell line, were purchased from ATCC and Jurkat cells, an immortalized line of human T lymphocyte, were purchased from Korean Cell Line Bank. These cell lines were cultured in RPMI containing 10% FBS and 1% P/S until used.

Cell viability assay

To examine the cytotoxicity of drug, we assessed cell viability. Cell counting kit-8 solution (CCK-8, Dojindo, Kumamoto, Japan) was

added to each well of cells treated as described above. After incubation for 1 hour 30 minutes at 37℃ in the dark, we measured the absorbance at 450 nm using a microplate reader (Versamax, Molecular Devices, CA, USA).

Cytokines, chemokines and MMPs assay

We collected the supernatants of cells treated as described above. The concentration of IL-6, MMP-1, MMP-3, CCL2, CXCL8, and CXCL10 were measured from FLS culture supernatants. The concentration of TNF-α, IL-1β, IL-6, and IL-10 were measured from culture supernatants of PBMCs. All analyses except IL-6 were performed using Magnetic Luminex Screening Assay multiplex kits (Luminex assay, R&D systems). IL-6 levels were measured using Human IL-6 DuoSet enzyme-linked immunosorbent assay (ELISA) kit (R&D systems) according to the manufacturer's instructions.

Western blot

FLS were washed once with PBS and lysed into RIPA buffer (ThermoFisher Scientific) containing Halt Protease and Phosphatase Inhibitor Cocktail (ThermoFisher Scientific). The amount of protein was quantified with BCA Protein Assay Kit (Pierce, Thermofisher Scientific). The same amounts of total protein lysate were separated by electrophoresis on Bolt 4-12% Bis-Tris Plus Gels (Invitrogen, Thermofisher Scientific). Then

proteins were transferred to nitrocellulose (NC) membrane and membranes were blocked with 3% skim milk for 1 hour in Tris-buffered saline containing 0.05% Tween 20 (TBST). Blocked membranes were washed with TBST and incubated with primary antibodies recognizing HDAC6 (Cell Signaling Technology, MA, USA), acetyl cortactin, cortactin (Upstate, Millipore, MA, USA), acetyl tubulin, α-tubulin (Sigma-Aldrich), ICAM-1, VCAM-1, and GAPDH (Santa Cruz, TX, USA) at 4℃ overnight. The membranes were washed with TBST and incubated with the horseradish peroxidase -conjugated anti-mouse or anti-rabbit immunoglobulin (secondary antibodies, Jackson Immuno Research Laboratories, PA, USA) for 2 hours at room temperature. Membrane-bound secondary antibodies were detected by chemiluminescent substrate (Elpis Biotech, Daejeon, Republic of Korea).

Adhesion assay

U937 cells and Jurkat cells were labeled with 5 μM calcein-AM (Molecular Probes, Thermofisher Scientific) at 37℃ for 30 minutes. Calcein-labeled cells were washed with prewarmed serum free RPMI and resuspended at a density of 1×10^6 cells/ml. Resuspended cells were added to untreated or drug-treated RA FLS and incubated at 37℃ for 1 hour. Each well was washed twice with PBS to remove unattached cells, and then cells were lysed with 0.1% triton X-100 (Sigma-Aldrich) in PBS. The fluorescence of U937 and Jurkat cells adhering to RA FLS were analyzed in SpectraMax

M5 (Molecular Devices) at an excitation wavelength of 494 nm and an emission wavelength of 517 nm.

Wound healing assay

Before HDAC6i treatment to RA FLS, cell monolayers were scraped using a sterile pipette tip and washed. The wounded cell layers were untreated or pretreated with HDAC6i prior to the stimulation of IL-1β. The images of wounded site were taken every 24 hours until reaching 72 hours using microscopy (DFC295, Leica, Wetzlar, Germany) and its software LAS V3.8 (Leica). Cells beyond guiding line were counted for quantification of data.

Induced Treg (iTreg) differentiation

CD4+CD25- T cells (Teff) were separated from PBMCs isolated from heparinized blood of RA patients using CD4+CD25+ Regulatory T Cell Isolation Kit, human (Miltenyi Biotec, Bergish Gladbach, Germany) according to the manufacturer's instructions. The purity of separated CD4+CD25- T cells (effector T cells, Teff) was >95% as confirmed by flow cytometry.

OKT3 anti-human CD3 monoclonal antibody (eBioscience, Thermofisher Scientific) was diluted into 2 μg/ml with PBS. Prepared anti-CD3 antibody solution was coated on 48-well plate for 2 hours at 37℃ with sealing. The coated plate was washed twice with PBS. Isolated CD4+CD25- T cells were resuspended in X-VIVO 15 (Lonza, Basel, Switzerland) containing 10% human serum

AB (Lonza) and 1% P/S with 2 μg/ml of anti-human CD28 antibody (BD Biosciences, CA, USA), 20 ng/ml of recombinant human IL-2 (Peprotech, NJ, USA), 5 ng/ml of recombinant human TGF-β (Peprotech), and 20 nM of 1,25-dihydroxyvitamin D_3 (Vitamin D_3, Sigma-Aldrich) at a density 1×10^6 cells/ml. Resuspended CD4+CD25- T cells were seeded in anti-CD3 antibody-coated plate with vehicle or HDAC6i and incubated for 5 days. After 5 days, iTreg were harvested and washed with PBS.

Flow cytometry

Anti-CD4-BV421, anti-CD25-BB515, anti-Foxp3-PE, and anti-CTLA-4-APC antibodies (BD Biosciences) were purchased. iTreg differentiated under different drug conditions were prepared separately. To block nonspecific binding of antibodies, FcR blocker (Miltenyi biotec) were added to each tube and incubated at 4℃ for 10 minutes. After washing with stain buffer (BD Biosciences), the cocktail of anti-CD4 and anti-CD25 antibody labeled with fluorescence were added to cell pellet and incubated at 4℃ for 30 minutes in the dark for surface staining. Surface-stained cells were washed twice with stain buffer. Intracellular staining for Foxp3 and CTLA-4 was performed using the Foxp3/Transcription Factor Staining Buffer set (eBioscience) according to manufacturer's instructions. Fluorescence-labeled iTreg were fixed with IC fixation buffer (eBioscience). The fluorescence of each marker was measured using LSR Fortessa X-20 (BD Bioscience) and data were

analyzed using Flowjo software (TreeStar, OR, USA).

Suppression assay

Suppression assay using human iTreg and Teff

CD4+CD25− T cells (Teff) were purified from healthy donor (HC) as described above. HC Teff were obtained from the identical healthy donor for consistency and labeled with Celltrace carboxyfluorescein succinimidyl ester (CFSE) cell proliferation kit (Molecular Probes) according to the manufacturer's instructions. CFSE−labeled HC Teff were cocultured with vehicle−treated or HDAC6i−treated RA iTreg. These cells were seeded in 96−well plate and incubated for 84 hours in the dark with Dynabeads human T−activator CD3/CD28 (ThermoFisher Scientific). Cell mixture were washed with PBS and fixed with IC fixation buffer. The proliferation of Teff was evaluated by CFSE dilution using LSR Fortessa X−20 (BD Biosciences) and the data were analyzed using Flowjo software (Treestar). The results were expressed as suppression rate (%) using the following formula [18]:

$$Suppression\ rate\ (\%) = \frac{(proliferation\ of\ Teff\ \ only) - (proliferation\ of\ Teff + Treg)}{(proliferation\ of\ Teff\ \ only)} \times 100$$

Suppression assay using murine Treg and Teff

Treg and Teff cells were isolated from splenocyte of naïve C57BL/6 mice using CD4+CD25+ regulatory T cell Isolation Kit (Miltenyi Biotec) by MACS separator according to the manufacturer's instructions. The purity of each cell population was > 95% as confirmed by flow cytometry. Then, Teff were labeled with 5 μM

Cell Proliferation Dye eFluor®670 (eBioscience) for 10 minutes at 37℃ under the protection from light. Treg were mixed with eFluor®670-labeled Teff at ratios of 0:1, 0.25:1 or 0.5:1 in RPMI containing 10% FBS, 1% P/S, 1 mM sodium pyruvate (Gibco), and 1% 2-mercaptoethanol (Gibco) in 96-well plate. The mixed cells were incubated with vehicle or HDAC6i in the presence of anti-CD3/CD28 beads (T cell Activation/Expansion kit, Miltenyi Biotec) for 4 days. The proliferation of Teff was anaylzed using LSR Fortessa (BD Bioscience). The results were anaylzed by FlowJo software. The results were expressed as suppression rate (%) using the same formula as above [18].

AIA animal model

Lewis rats (female, 5 week) were purchased from Central Lab Animal, Inc. (Seoul, Republic of Korea) and kept for 1 week before the test. Animals were provided with standard diet (Central Lab Animal, Inc.) and water *ad libitum* and housed in controlled environment with temperature (22 ± 2℃), humidity (44-56%) and 12 hours light-dark cycle. Complete Freund's adjuvant (CFA, Chondrex, WA, USA) was resuspended vigorously. A 100 μL of CFA was injected subcutaneously into a base of tail for AIA induction. After 7 days of induction, animals were divided into 6 groups (8 or 9 animals per group). Each group was treated with vehicle or M808 once a day orally. Clinical score of arthritis and body weight were measured at day 9, 13 and 17 after induction.

The severity of arthritis was evaluated by clinical scoring of each joint considering joint swelling and erythema (score 0 to 4). The clinical scores for four joints were summed up to give the total score of each animal [15].

Statistical analysis

All human data are presented as the mean±SEM and all animal data are presented as the mean±SD. Two-tailed paired Wilcoxon signed rank test were used for statistical analysis of all human data and two-tailed Mann-Whitney test or paired t-test were used for statistical analysis of animal data using GraphPad Prism 5 (GraphPad, CA, USA). Statistical significance was considered at $p < 0.05$.

Results

In vitro selectivity of M808 for HDAC6

To examine whether M808 is a HDAC6-specific inhibitor or not, the half maximal inhibitory concentrations (IC_{50}) test was performed. LBH589, a pan-HDACi, influenced on nine HDACs in a range under 15 μM. In contrast, M808 showed HDAC6-specific inhibition by presenting definitely lower IC_{50} value in HDAC6 than other HDAC series, even compared to ACY1215, a commercial HDAC6i (Table 1). This result showed that M808 is a HDAC6 selective inhibitor.

Effects of M808 on the production of cytokines and MMPs in RA FLS

We examined whether M808 affect the expression of IL-6, MMP-1, and MMP-3 in RA FLS. To exclude the potential toxic effects of HDAC6i on FLS, cell viability assay was performed using CCK-8 assay. RA FLS untreated or treated with HDAC6i were stimulated with IL-1β for 24 hours. The viability of RA FLS was not affected by tubastatin A or M808 (Figure 1A). The expression in IL-6, MMP-1, and MMP-3 were measured in the culture supernatants of RA FLS treated with M808 as described above by Luminex assay and ELISA. In M808-treated RA FLS, IL-1β-induced expression of IL-6, MMP-1, and MMP-3 were significantly decreased while

tubastatin A only decreased MMP-3 (Figure 1B-D). These data suggest that M808 prevent RA FLS from secretion of pro-inflammatory cytokines and MMPs with better efficiency than tubastatin A.

M808 suppressed cell migration and deacetylation of tubulin and cortactin

Tubulin and cortactin have been reported as the substrates of HDAC6 and were also known as related molecules with cytoskeleton such as microtubule and F-actin, respectively [19, 20]. We assessed the expression of HDAC6, acetylated tubulin, and acetylated cortactin using western blot in RA FLS after M808 treatment. The higher concentration of M808 was exposed to RA FLS, the more increased levels of acetylated tubulin and acetylated cortactin were detected. Tubastatin affected only tubulin acetylation. The protein expression of HDAC6 did not change in all conditions (Figure 2A). In addition, we investigated whether cell migration is regulated by the presence of M808 in RA FLS using wound healing assay. RA FLS were treated with M808 before IL-1β stimulation as described above. The extended incubation time upto 72 hours did not influence on cell viability of FLS (Figure 2B). Cell migration decreased dose-dependently in M808-treated RA FLS although there was no the difference of cell migration between vehicle group and IL-1β-stimulated group (Figure 2C-D). These data indicate that M808 increases the acetylation of tubulin and cortactin and

impedes cell migration of RA FLS.

M808 inhibited cell adhesion of U937 or Jurkat cell to FLS through the downregulation of ICAM-1 and VCAM-1

We next investigated the leukocyte adhesion on RA FLS. IL-1β-induced secretion of chemokines such as CCL2, CXCL8 and CXCL10 were significantly decreased in culture supernatants from RA FLS treated with M808 (Figure 3A-C). We also analyzed the secretion of CCL19, CCL21, CCL25, CXCL9, and CXCL11. CCL25, CXCL9, and CXCL11 were undetectable and CCL19 and CCL21 did not change after treatment with M808 (data not shown). In HDAC6i-treated RA FLS, IL-1β-induced expression of ICAM-1 and VCAM-1 were reduced in a dose-dependent manner (Figure 3D). Cell adhesion assay was conducted to further examine whether the decreased expression of adhesion molecules and chemokines modulate leukocyte adhesion. U937 cells, a human monocyte cell line, and Jurkat cells, a human T lymphocyte cell line, were used for the assessment of the adhesion of each cell type, monocytes and T cells respectively. In the experiment using U937 cells, IL-1β significantly increased cell adhesion to RA FLS, which was inhibited by M808 treatment (Figure 3E, left panel). Jurkat cells showed the similar adhesion pattern to U937 cell (Figure 3E, right panel). Taken together, M808 is able to control leukocyte adhesion to RA FLS by preventing IL-1β-induced expression of adhesion

molecules such as ICAM-1 and VCAM-1 as well as chemokines such as CCL2, CXCL8, and CXCL10, suggesting that M808 may reduce leukocyte infiltration to RA synovium.

Effects of M808 on the cytokine secretion in RA PBMCs

We examined whether M808 affect on pro- or anti- inflammatory cytokines in RA PBMCs. PBMCs were isolated from heparinized blood of RA patients and treated with vehicle or HDAC6i followed by LPS stimulation. To identify potential cytotoxic effect of M808 on PBMCs, we first performed cell viability assay. HDAC6i-treated PBMCs did not show any change in cell viability (Figure 4A). To further determine whether M808 regulate the expression of cytokines in RA PBMCs, the secretion of TNF-α, IL-1β, IL-6, and IL-10 was measured in culture supernatants of RA PBMCs using Luminex assay and ELISA. M808 significantly decreased the level of TNF-α (Figure 4B) and increased the level of IL-10, an anti-inflammatory cytokine (Figure 4E) whereas those of IL-1β and IL-6 showed no significant change (Figure 4C-D). These data indicate that M808 mitigates LPS-induced inflammatory responses in RA PBMCs by suppressing TNF-α expression and promoting IL-10 expression.

Effects of M808 on the expression of Treg markers in

iTreg from RA PBMCs

We investigated whether M808 enhance Treg markers such as Foxp3 and CTLA-4 in RA Treg. iTreg were induced from CD4+CD25- T cells isolated from RA PBMCs in the differentiation medium containing anti-CD3/CD28 antibodies, IL-2, TGF-β, and vitamin D_3 in the presence or absence of HDAC6i. The percentage of CD4+CD25+Foxp3+ cells in total cells were defined as the differentiation rate into iTreg and the rate was decreased in 2 μM of M808-treated group (Figure 5A). M808-treated iTreg showed comparable expression of Foxp3 and CTLA-4 to vehicle-treated iTreg (Figure 5B). We then determined the density of each marker on iTreg and undifferentiated cells (CD4+CD25-) by analyzing mean fluorescence intensity (MFI). There was no significant difference of Foxp3 and CTLA-4 on iTreg in MFI between vehicle and HDAC6i-treated groups (Figure 5C). Interestingly, CTLA-4 expression in CD4+CD25- T cells were significantly increased in M808-treated groups in a dose-dependent manner (Figure 5D). Therefore, M808 does not increase the differentiation rate into iTreg and the expression of Treg markers in iTreg, but enhances the expression of CTLA-4 in CD4+CD25- T cells.

Effects of M808 on the suppressive function of iTreg from RA PBMCs

We examined whether M808 have suppressive effects on proliferation of Teff. iTreg from RA patients were prepared under

the treatment of vehicle or HDAC6i as described above. Before the coculture with RA iTreg, HC Teff were labeled with CFSE to estimate Teff proliferation by assessing the division of CFSE-labeled cells. As we found that both tubastatin A and M808 suppressed HC Teff proliferation without Treg (data not shown), HDAC6i were not treated during coculture period. The proliferation of Teff cells were recalculated as suppression rate using the formula described in methods. iTreg differentiated with M808 displayed the enhanced suppressive function compared to iTreg treated with vehicle or tubastatin A (Figure 6A-C). Suppression rate was increased as the proportion of Treg in cocultured cells increased (Figure 6B). These data demonstrate that M808 leads iTreg from RA patients to improve the suppressive function.

Suppressive function of M808 on murine T cells

We next examined whether murine Treg have the same tendency to suppress the proliferation of Teff as human iTreg under the treatment of M808. The suppression rate was calculated using the proliferation of Teff as described. The suppression rate was increased in M808-treated groups dose-dependently (Figure 7A-B). When we cultured Teff only with M808, M808 decreased the proliferation of Teff, which means M808 could suppress murine Teff itself. Moreover, coculturing Teff and Treg with M808 significantly increased the suppression rate compared to culturing Teff and Treg with vehicle. These data suggest that M808 is

capable of suppressing the proliferation of Teff and enhancing the suppressive function of Treg.

Effects of M808 on AIA

To investigate the effects of M808 *in vivo*, we induced AIA model in Lewis rat by injection of CFA on day 0. Vehicle or M808 was administered orally every day after a week from induction. The dosage range of M808 was 3 mg/kg to 100 mg/kg and each group consisted of nine except the group of 50 mg/kg (n = 8). Body weight and clinical score were monitored at day 9, 13 and 17. Clinical score was graded based on arthritic severity such as joint edema and erythema. At day 17 after AIA induction, the loss of body weight significantly recovered in 30 and 100 mg/kg of M808-treated group (Figure 8A). The clinical score of arthritis was significantly decreased (Figure 8B).

IC_{50}	LBH-589	ACY1215	CKD-M808
HDAC1	**3.8**	**480**	**3840**
HDAC2	**12.0**	**2050**	**2200**
HDAC3	**4.8**	**2140**	**6360**
HDAC4	**120.0**	**5220**	**ND**
HDAC5	**6.3**	**7400**	**ND**
HDAC6	**3.2**	**10.0**	**4**
HDAC7	**12.7**	**8050**	**ND**
HDAC8	**53.0**	**240**	**1380**
HDAC9	**8.6**	**10000**	**ND**
HDAC10	**8.7**	**6100**	**ND**
HDAC11	**7.8**	**2580**	**120**

Table 1. CKD-M808 is a selective HDAC6 inhibitor.

To confirm *in vitro* selectivity, IC_{50} values for HDAC family members were measured using HDACi. The unit of each value is μM. CKD-M808 showed remarkably lower IC_{50} value toward HDAC6 compared to the value toward other HDAC family. IC_{50} value of CKD-M808 toward HDAC6 was even lower than other HDAC6i, ACY1215. LBH589, a pan-HDACi, and ACY1215 were used as reference groups. (ND = not determined)

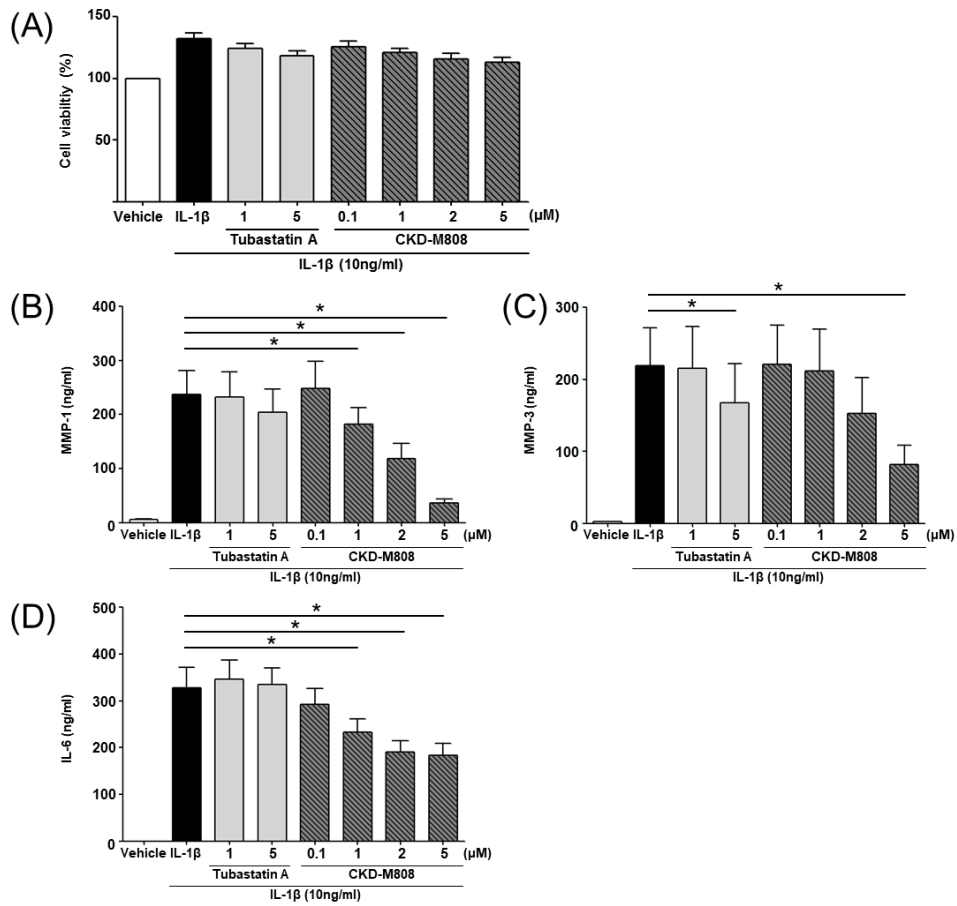

Figure 1. CKD-M808 suppressed the secretion of MMP-1, MMP-3, and IL-6 in RA FLS.

RA FLS (n = 6) were pretreated with HDAC6i (tubastatin A or M808) for 1 hour, then stimulated for 24 hours with IL-1β. (A) M808 had no significant effect on the viability of RA FLS. The production of (B) MMP-1, (C) MMP-3, and (D) IL-6 were decreased in a dose-dependent manner. Data are presented as the mean±SEM. * $p < 0.05$, as compared with the cells stimulated with IL-1β after vehicle treatment using Wilcoxon signed rank test.

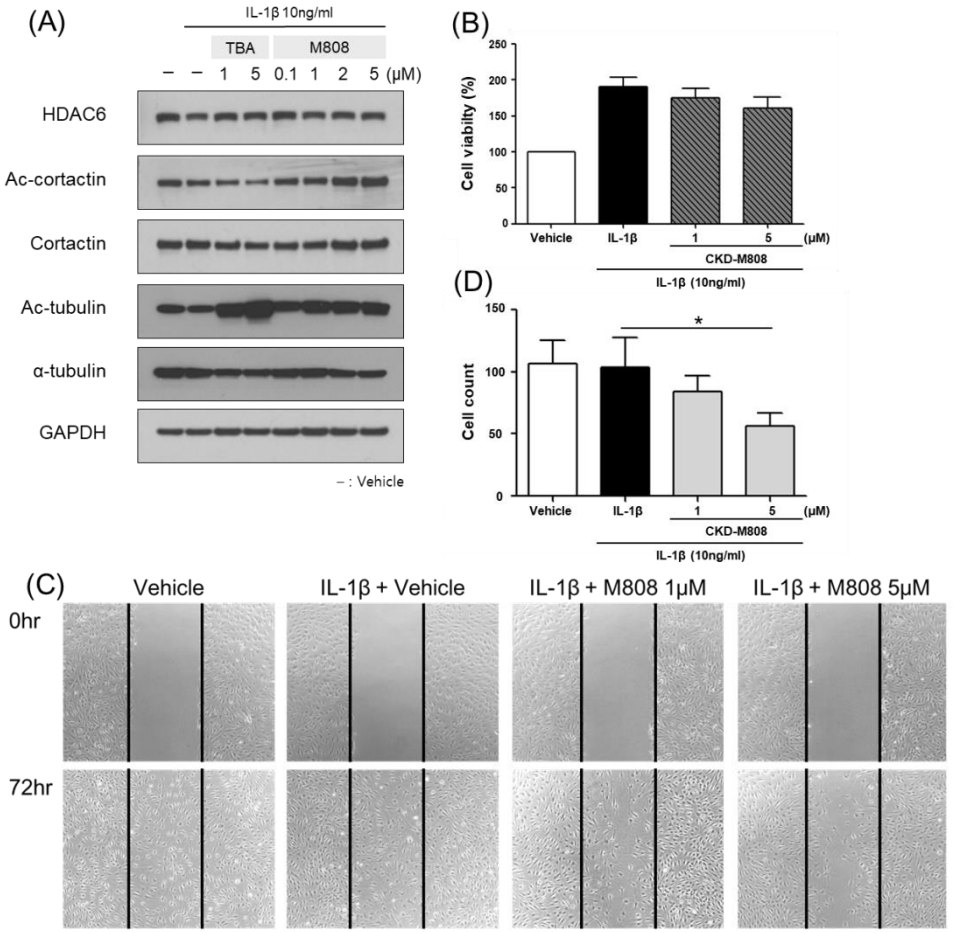

Figure 2. CKD-M808 induced the acetylation of tubulin and cortactin in FLS with less cell migration of FLS.

RA FLS were pretreated with HDAC6i (tubastatin A or M808) for 1 hour, followed by the stimulation of IL-1β for 24 hours. (A) The levels of acetylation of tubulin and cortactin in RA FLS were analyzed via western blot. Data shown are representative of experiments from three different RA patients. To evaluate the migration ability of the cells, wound healing assay was performed. For wound healing assay, RA FLS (n = 6) were pretreated with M808 for 1 hour, followed by stimulation of IL-1β for 72 hours. (B)

Despite no significant change of cell viability, (C-D) cell migration dose-dependently decreased in M808-treated RA FLS. (C) Data shown are representative of experiments from six different RA patients. Original magnification is ×40. (D) Cells migrating beyond the black line of microscopy images were counted. TBA is the abbreviation of tubastatin A. Data are presented as the mean±SEM. * $p < 0.05$, as compared with the cells stimulated with IL-1β after vehicle treatment using Wilcoxon signed rank test.

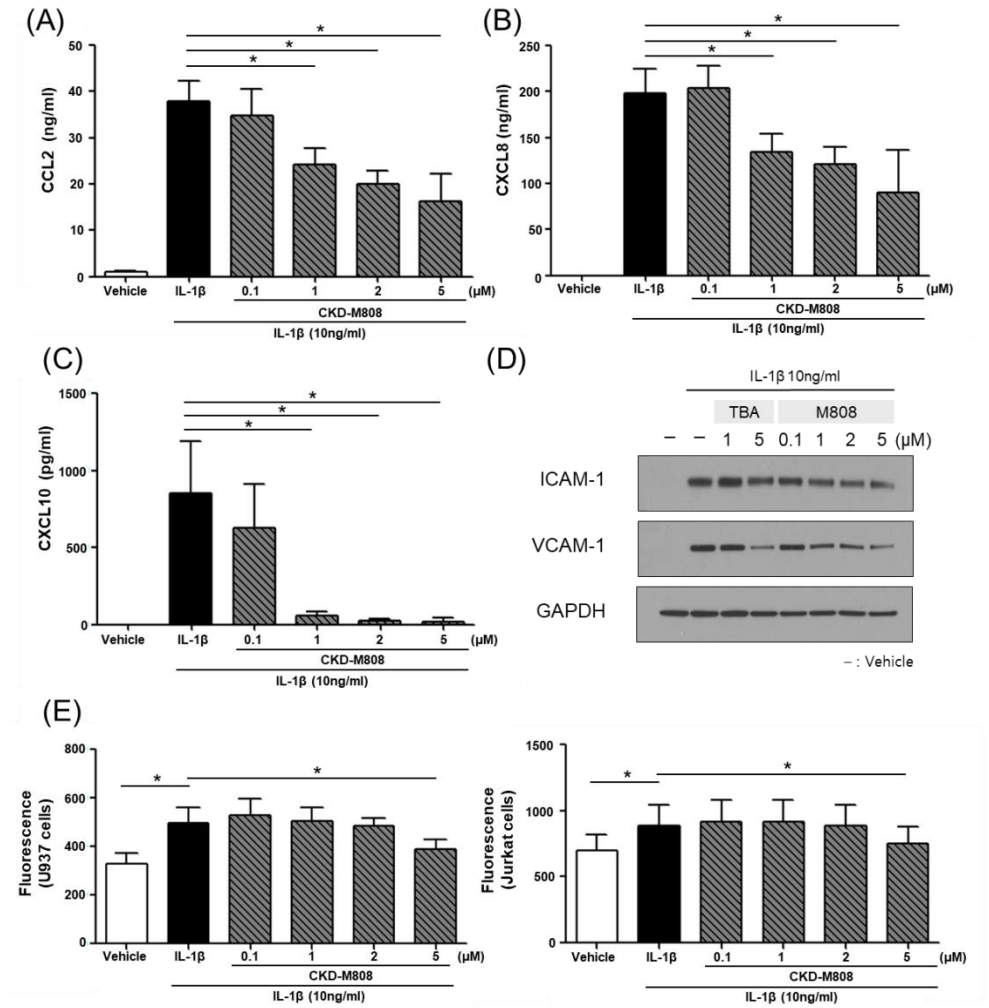

Figure 3. CKD-M808 decreased cell adhesion by downregulating the expression of adhesion molecules and chemokines in RA FLS.

RA FLS were pretreated with HDAC6i (tubastatin A or M808) for 1 hour, followed by stimulation of IL-1β for 24 hours. (A-C) The levels of chemokines secreted from RA FLS were analyzed by Luminex assay. (D) The expression levels of ICAM-1 and VCAM-1 were detected by western blot. Data shown are representative of experiment from three different RA patients. To confirm monocyte or T cell adhesion to M808-treated RA FLS, cell adhesion assay

was performed (n = 6). (E) The adhesion of calcein-labeled U937 (left panel) and Jurkat cells (right panel) to RA FLS were evaluated by measuring fluorescent intensity of calcein. TBA ; tubastatin A. Data are presented as the mean±SEM. * $p < 0.05$, as compared with the cells stimulated with IL-1β after vehicle treatment using Wilcoxon signed rank test.

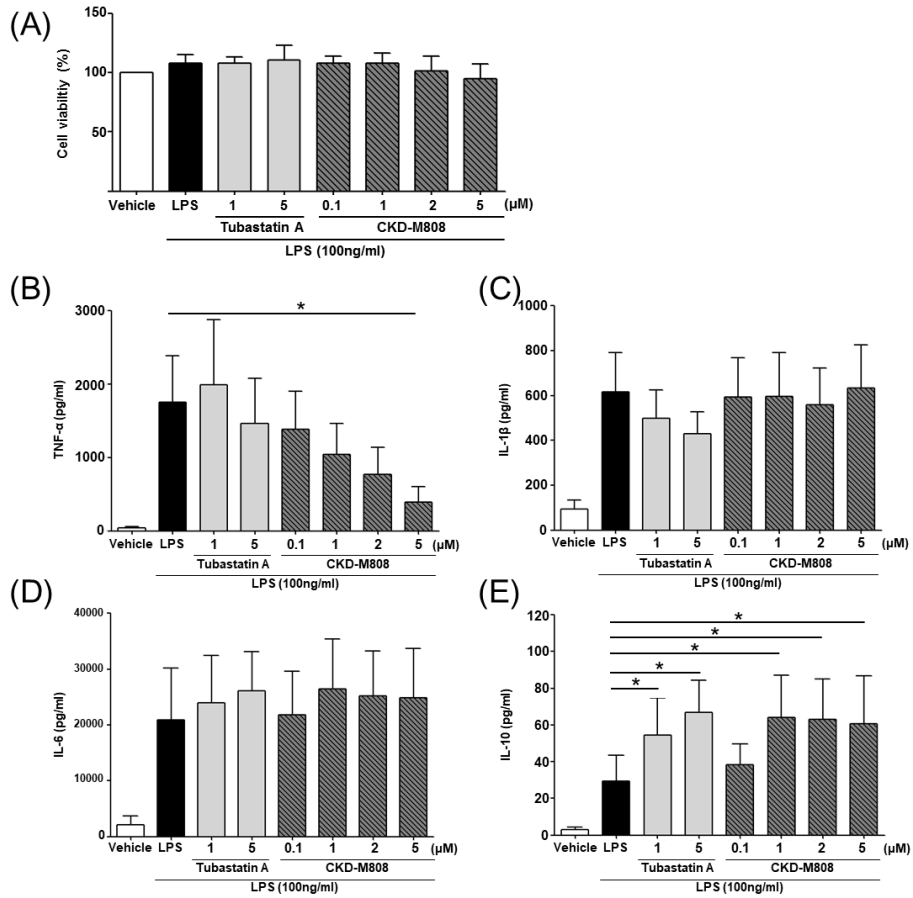

Figure 4. CKD-M808 suppressed TNF-α and enhanced IL-10 production, but did not affect cell viability in RA PBMCs.

RA PBMCs (n = 6) were pretreated with HDAC6i (tubastatin A or M808) for 1 hour, then stimulated for 24 hours with LPS. (A) M808 showed no significant cytotoxicity in RA PBMCs. M808 suppressed the level of (B) TNF-a, but had negligible effects on the levels of (C) IL-1β and (D) IL-6. (E) The level of IL-10 was enhanced in M808-treated RA PBMCs. Data are presented as the mean±SEM. * $p < 0.05$, as compared with the cells stimulated with LPS after vehicle treatment using Wilcoxon signed rank test.

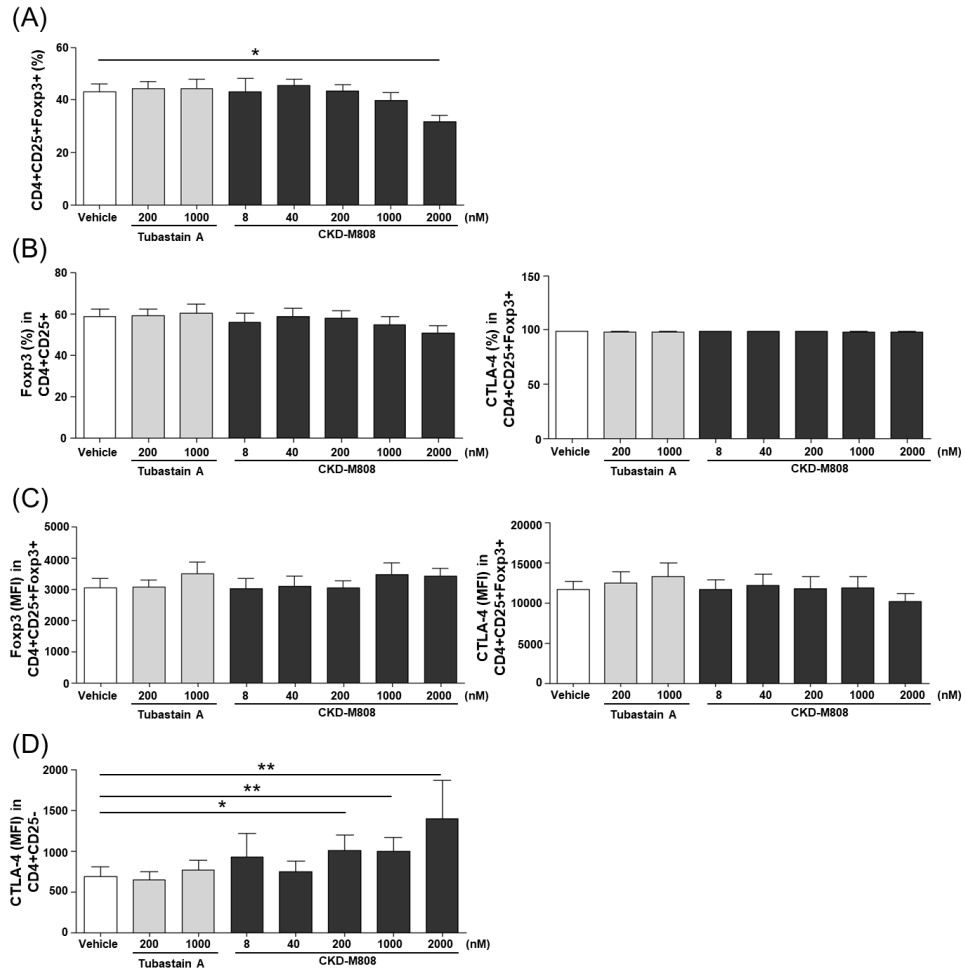

Figure 5. CKD-M808 increased the expression of CTLA-4 in CD4+CD25- cells but not in CD4+CD25+Foxp3+ cells.

CD4+CD25- T cell from RA PBMCs (n = 7 for tubastatin A group, n = 8 for vehicle and M808 group) were differentiated into iTreg in the presence of vehicle or HDAC6i. (A) The differentiation rate into CD4+CD25+Foxp3+ cells (iTreg) was analyzed by flow cytometry. (B) The frequencies of Foxp3 and CTLA-4 in iTreg were not different in all conditions. Mean fluorescence intensity (MFI) of Treg markers in (C) iTreg and (D) CD4+CD25- T cells were analyzed by flow cytometry. Data are presented as the mean±SEM.

* $p < 0.05$, ** $p < 0.01$ as compared with the cells treated with vehicle using Wilcoxon signed rank test.

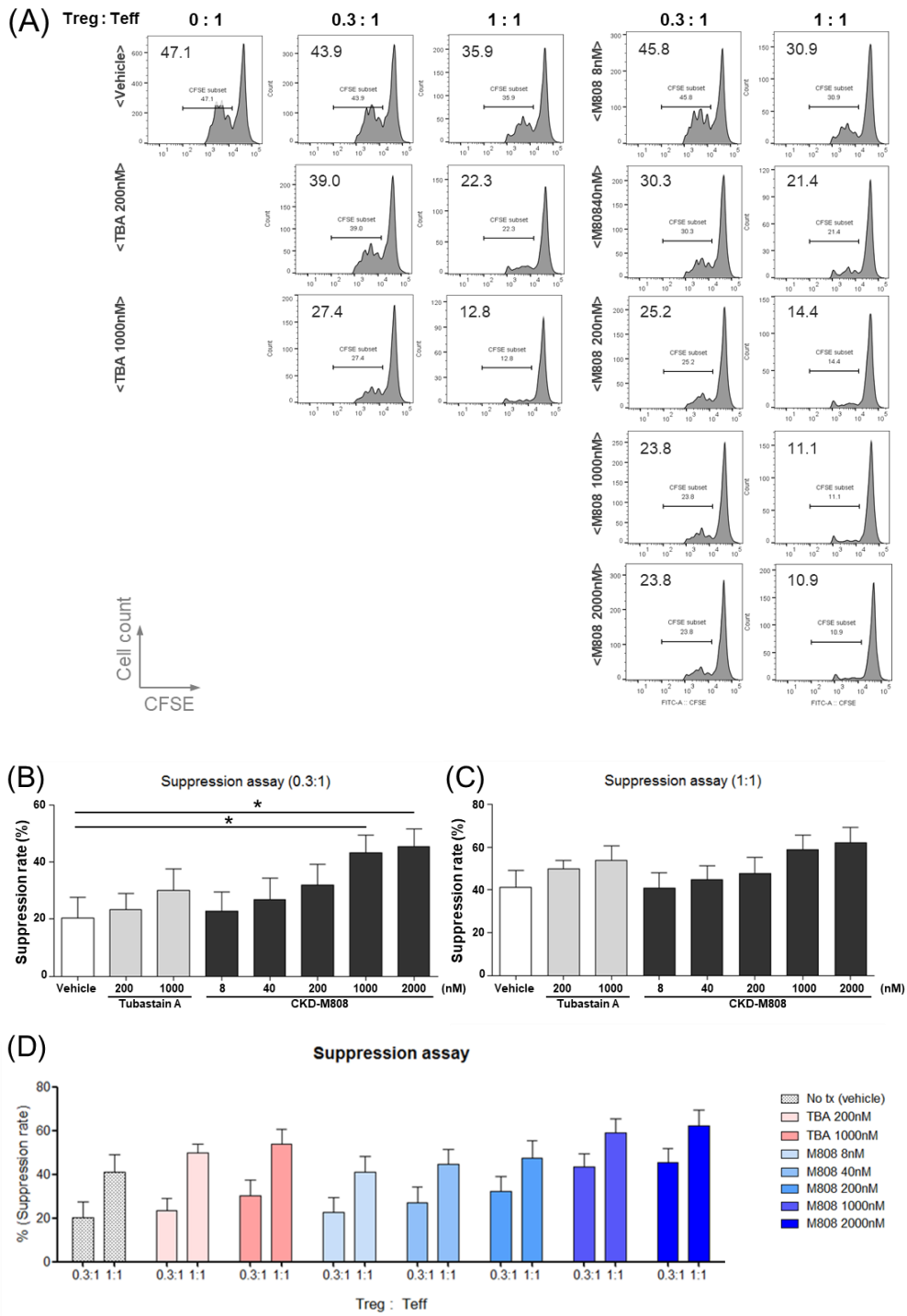

Figure 6. CKD-M808 improved suppressive function of iTreg

To examine the suppressive function of iTreg, suppression assay were conducted. iTreg from RA patients differentiated in the

presence or absence of HDAC6i and incubated with Teff from healthy donor for 84hrs (n = 6 for tubastatin A group, n = 7 for vehicle and M808 groups). (A) is the representative graph which shows the percentages of the proliferation of Teff labeled with CFSE. The number of upper left is the proliferation rate of Teff. (B-C) The suppression rate was calculated according to the concentration of M808 as described in methods. (D) is suppression rate according to the ratio of iTreg and Teff. TBA ; tubastatin A. Data are presented as the mean±SEM. * $p < 0.05$, as compared with the cells treated with vehicle using Wilcoxon signed rank test.

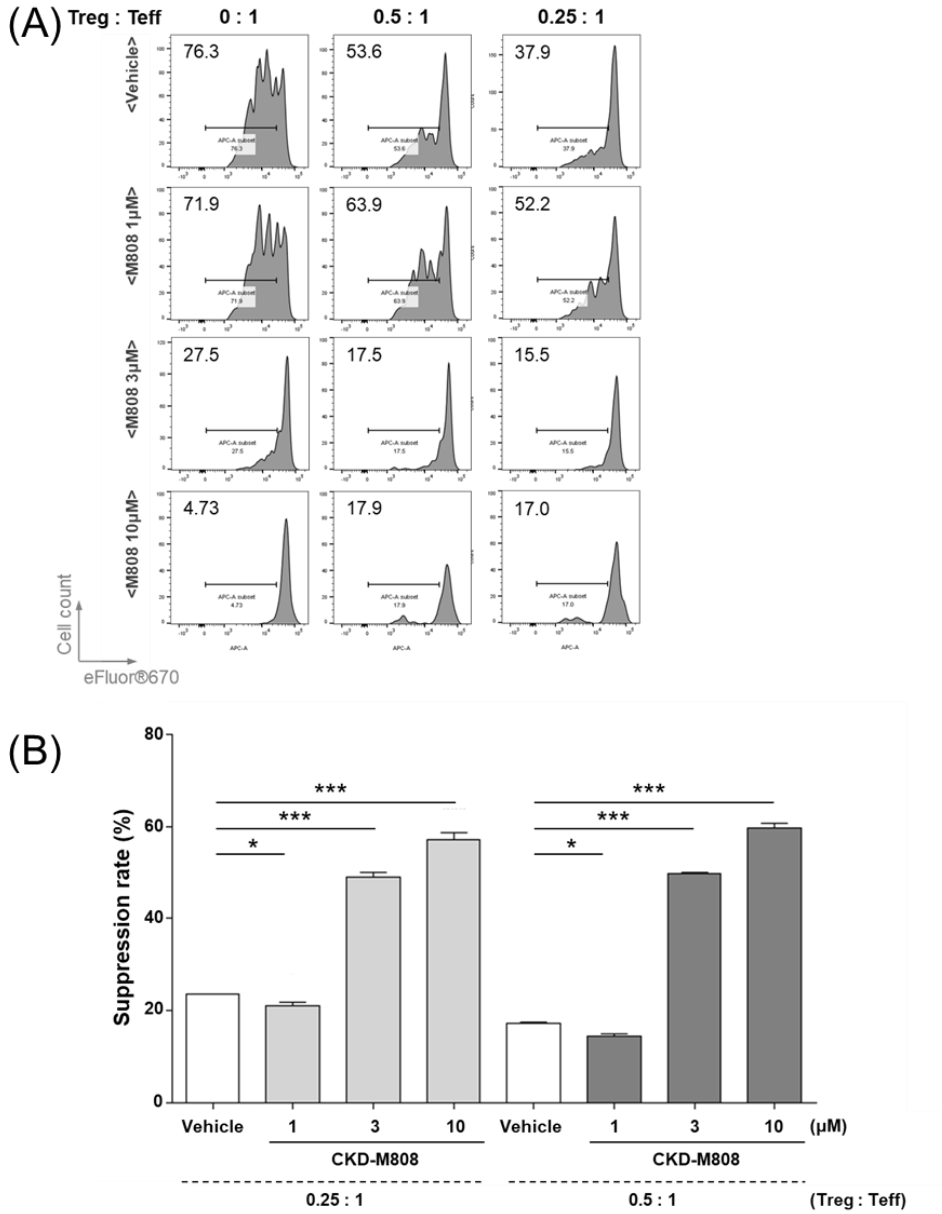

Figure 7. CKD-M808 enhanced suppressive function of mouse Treg.

Murine Treg and Teff were incubated with vehicle or M808 for 4 days (n = 3). (A) The data are the representative graph which shows the percentages of proliferation of Teff labeled with eFlour®670. The number of upper left is the proliferation rate of Teff. (B) The suppression rate was calculated as described.

Suppression rate was increased in the presence of M808. Data are presented as the mean±SD. * $p < 0.05$, *** $p < 0.001$ as compared with the cells treated with vehicle using paired t-test.

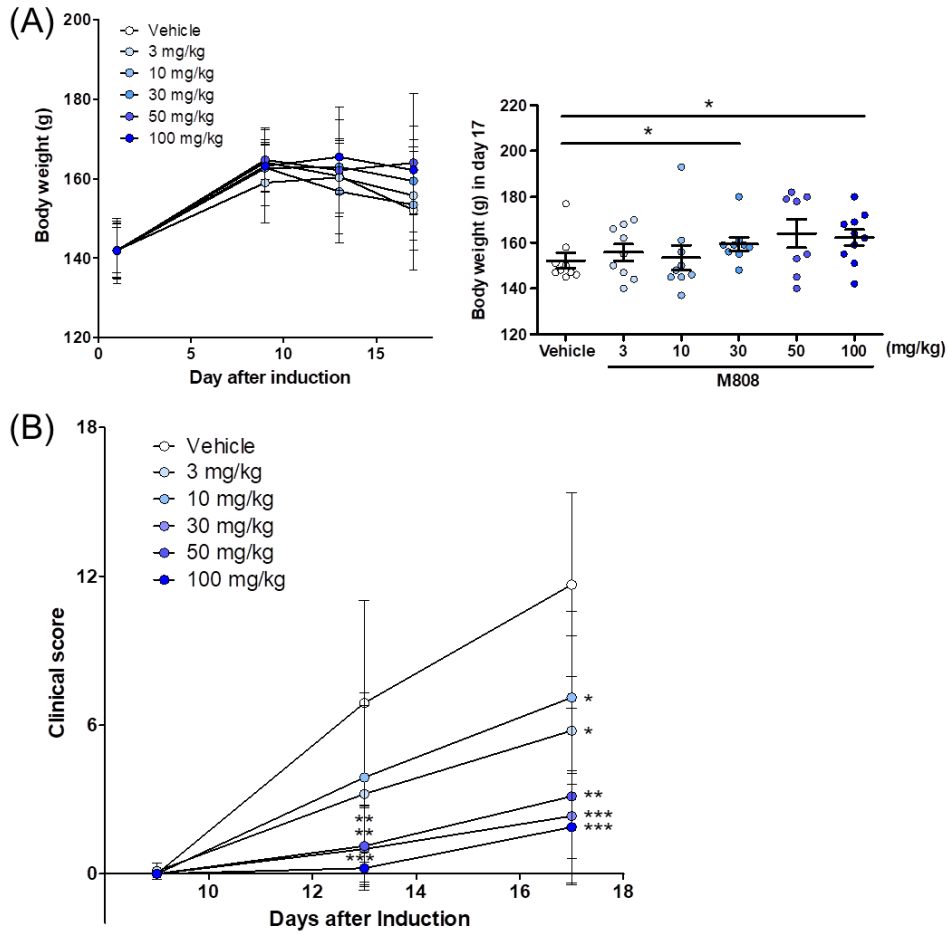

Figure 8. CKD-M808 increased body weight and decreased clinical score of arthritis in AIA model.

AIA was induced in Lewis rats as described in method. Vehicle (n = 9) or M808 (3, 10, 30, 50 and 100 mg/kg, n = 9, 9, 9, 8 and 9, respectively) was administered daily after a week from AIA induction. Body weight and clinical score of arthritis were measured at day 9, 13 and 17 after induction. (A) Body weight was increased with the treatment of M808. (B) Clinical score of arthritis at day 13 and 17 were decreased dose-dependently in M808-treated groups compared to vehicle group. Data are presented as the mean±SD.

* $p < 0.05$, ** $p < 0.01$, *** $p < 0.001$, as compared with vehicle group using Mann-Whitney test.

Discussion

In treatment of RA, efficacy and safety issues of available current therapies such as DMARDs and biologics have continued, emphasizing the necessity of novel therapeutic reagent. HDACs are related to pathogenesis of diseases such as cancer, neurological diseases, and immune disorders and pan-HDACi was reported as competent drugs in these diseases through the epigenetic regulation [21]. Despite this efficacy, pan-HDACi had unexpected side effects including fatigue, diarrhea, and thrombocytopenia in recent clinical trials [13]. Consequently, the development of selective HDACi was promoted and expected to have similar pharmaceutical efficacy to pan-HDACi with more safety. Here we investigated that a novel HDAC6i, M808 could have a similar therapeutic effects in FLS, PBMCs, iTreg of RA patients, and animal models as previously reported for pan-HDACi.

FLS play an essential role in inflammation in RA by producing pro-inflammatory cytokines such as TNF-α or IL-6 and tissue degrading factor such as MMPs [22]. Tubastatin A, a well-known HDAC6i, attenuated synovial inflammation and reduced the level of IL-6 in sera of collagen antibody-induced arthritis (CAIA) mouse model in a previous study [23]. In synovium-derived RA FLS, M808 inhibited the production of pro-inflammatory cytokines and proteases such as IL-6, MMP-1 and MMP-3.

Hyperproliferation of FLS and abundant infiltration of leukocyte

are distinguishing pathological phenomenon of RA [24]. In previous studies, the acetylation of microtubule is responsible for decrease in cell migration and invasion in various cell type such as neurons and endothelial cells [25-27] and acetylated cortactin regulates cell migration in NIH 3T3 cells and endothelial cells [28, 29]. In our study, extensive increase in acetylation levels of tubulin and cortactin was observed in RA FLS incubated with M808, which may contribute to impede cell migration of FLS.

Leukocyte migration into infected or injured sites is a prerequisite step for fundamental immune responses. The recruitment of leukocyte to inflamed tissues plays a central role in the progress of RA [7, 30]. It has been previously reported that tubastatin A represses the expression of TNF-α-induced ICAM-1 and VCAM-1 [31] and tubastatin A regulates the production of CCL2, CXCL8, and CXCL10 in astrocytes [32]. In our study, M808 decreased IL-1β-induced production of adhesion molecules and chemokines in RA FLS. Consistent with this data, M808 suppressed the adhesion of monocytes or T lymphocytes on RA FLS. Leukocyte retention and infiltration may be reduced in accordance with decline in leukocyte recruitment and adhesion, consequentially leading to repress synovial inflammation.

In recent studies, tubastatin A displayed anti-inflammatory effects in CIA mouse model and inhibited TNF-α and IL-6 secretion in human macrophage cell line, THP-1 cells [15]. Similarly, M808 also reduced the level of TNF-α and increased

the level of IL-10 in PBMCs from RA patients in this study. In addition, polarized activation into Teff such as T_H1 or T_H17 triggers immuno-inflammatory response in RA [7]. To prevent excessive T cell activation and differentiation into Teff which is inducing self-destructive immune response, Treg suppress those activities of T cell [33]. Immune suppressive function of Treg is attributed to Treg markers such as Foxp3 and CTLA-4 [34, 35]. In a previous study, it was found that abundant Foxp3 protein and more acetylated Foxp3 were expressed in HDAC6 knockout mice [36]. The differentiation rate into iTreg and the expression of immunosuppressive markers of Treg including Foxp3 and CTLA-4 did not increase in iTreg under M808 treatment in the present study. However, iTreg differentiated under the presence of M808 had significantly enhanced suppressive function despite no change in iTreg markers. The expression level of CTLA-4 increased in CD4+CD25- cells. Therefore, there may be other markers expressed on Treg besides what we already examined, for example, GITR and PD-1. IL-10 or TGF-β may be responsible for HDAC6i-mediated increase in suppressive function of Treg. The mechanism of suppressive function of Treg by HDAC6i needs further investigation.

Even though we showed the therapeutic effects of M808 on RA FLS, we did not clarify the mechanisms associated M808-dependent regulation in cytokines, chemokines, and adhesion molecules. In a previous study, upregulated production of ICAM-1

and VCAM-1 by TNF-α were restored under the presence of mitogen-activated protein kinase (MAPK) inhibitors and NF-κB inhibitor, involving the potential connection between adhesion molecules and MAPK or NF-κB signaling [31]. Another possibility for the mechanisms is the regulation of adhesion molecule by the acetylation of cortactin. According to a recent study, cortactin phosphorylation by Src kinase can occur only in its deacetylated state, implying the acetylation state is inactive and stable [37]. Additionally, phosphorylation of cortactin by Src kinase is responsible for the clustering of E-selectin and ICAM-1 in endothelial cells [38]. Taken together, we can speculate that HDAC6i may regulate ICAM-1 with acetylated cortactin which may block cortactin phosphorylation. To confirm these hypotheses, further study is required.

In summary, this study demonstrated that a novel HDAC6i, M808 had an impact on inflammatory activation of RA FLS through not only the downregulation of pro-inflammatory cytokines, chemokines, and MMPs but also the inhibition of excessive cell migration and adhesive capacity. M808 also regulated the cytokines associated with immune responses in RA PBMCs. Treg induced from RA PBMCs showed the improved suppressive ability in the presence of M808 and the proliferation of murine Teff was decreased when M808 was treated. Furthermore, M808 showed therapeutic effects in AIA animal model by restoring body weight loss and improving clinical score. M808, a selective HDAC6i, may

provide a new therapeutic option for RA patients.

References

1. de Ruijter AJ, van Gennip AH, Caron HN, Kemp S, van Kuilenburg AB: Histone deacetylases (HDACs): characterization of the classical HDAC family. *Biochem J* 2003, 370(Pt 3):737-749.
2. Bannister AJ, Kouzarides T: Regulation of chromatin by histone modifications. *Cell Res* 2011, 21(3):381-395.
3. Li Y, Shin D, Kwon SH: Histone deacetylase 6 plays a role as a distinct regulator of diverse cellular processes. *FEBS J* 2013, 280(3):775-793.
4. Aldana-Masangkay GI, Sakamoto KM: The role of HDAC6 in cancer. *J Biomed Biotechnol* 2011, 2011:875824.
5. Dompierre JP, Godin JD, Charrin BC, Cordelieres FP, King SJ, Humbert S, Saudou F: Histone deacetylase 6 inhibition compensates for the transport deficit in Huntington's disease by increasing tubulin acetylation. *J Neurosci* 2007, 27(13):3571-3583.
6. de Zoeten EF, Wang L, Butler K, Beier UH, Akimova T, Sai H, Bradner JE, Mazitschek R, Kozikowski AP, Matthias P *et al*: Histone deacetylase 6 and heat shock protein 90 control the functions of Foxp3(+) T-regulatory cells. *Mol Cell Biol* 2011, 31(10):2066-2078.
7. Smolen JS, Steiner G: Therapeutic strategies for rheumatoid arthritis. *Nat Rev Drug Discov* 2003, 2(6):473-488.

8. Kawabata T, Nishida K, Takasugi K, Ogawa H, Sada K, Kadota Y, Inagaki J, Hirohata S, Ninomiya Y, Makino H: Increased activity and expression of histone deacetylase 1 in relation to tumor necrosis factor-alpha in synovial tissue of rheumatoid arthritis. *Arthritis Res Ther* 2010, 12(4):R133.
9. Grabiec AM, Reedquist KA: The ascent of acetylation in the epigenetics of rheumatoid arthritis. *Nat Rev Rheumatol* 2013, 9(5):311-318.
10. Cantley MD, Bartold PM, Fairlie DP, Rainsford KD, Haynes DR: Histone deacetylase inhibitors as suppressors of bone destruction in inflammatory diseases. *J Pharm Pharmacol* 2012, 64(6):763-774.
11. Sweet MJ, Shakespear MR, Kamal NA, Fairlie DP: HDAC inhibitors: modulating leukocyte differentiation, survival, proliferation and inflammation. *Immunol Cell Biol* 2012, 90(1):14-22.
12. Grabiec AM, Korchynskyi O, Tak PP, Reedquist KA: Histone deacetylase inhibitors suppress rheumatoid arthritis fibroblast-like synoviocyte and macrophage IL-6 production by accelerating mRNA decay. *Ann Rheum Dis* 2012, 71(3):424-431.
13. Subramanian S, Bates SE, Wright JJ, Espinoza-Delgado I, Piekarz RL: Clinical Toxicities of Histone Deacetylase Inhibitors. *Pharmaceuticals (Basel)* 2010, 3(9):2751-2767.
14. Zhang Y, Kwon S, Yamaguchi T, Cubizolles F, Rousseaux S,

Kneissel M, Cao C, Li N, Cheng HL, Chua K *et al*: Mice lacking histone deacetylase 6 have hyperacetylated tubulin but are viable and develop normally. *Mol Cell Biol* 2008, 28(5):1688-1701.

15. Vishwakarma S, Iyer LR, Muley M, Singh PK, Shastry A, Saxena A, Kulathingal J, Vijaykanth G, Raghul J, Rajesh N *et al*: Tubastatin, a selective histone deacetylase 6 inhibitor shows anti-inflammatory and anti-rheumatic effects. *Int Immunopharmacol* 2013, 16(1):72-78.

16. Oh BR, Suh DH, Bae D, Ha N, Choi YI, Yoo HJ, Park JK, Lee EY, Lee EB, Song YW: Therapeutic effect of a novel histone deacetylase 6 inhibitor, CKD-L, on collagen-induced arthritis in vivo and regulatory T cells in rheumatoid arthritis in vitro. *Arthritis Res Ther* 2017, 19(1):154.

17. Arnett FC, Edworthy SM, Bloch DA, McShane DJ, Fries JF, Cooper NS, Healey LA, Kaplan SR, Liang MH, Luthra HS *et al*: The American Rheumatism Association 1987 revised criteria for the classification of rheumatoid arthritis. *Arthritis Rheum* 1988, 31(3):315-324.

18. Peres RS, Liew FY, Talbot J, Carregaro V, Oliveira RD, Almeida SL, Franca RF, Donate PB, Pinto LG, Ferreira FI *et al*: Low expression of CD39 on regulatory T cells as a biomarker for resistance to methotrexate therapy in rheumatoid arthritis. *Proc Natl Acad Sci U S A* 2015, 112(8):2509-2514.

19. Hubbert C, Guardiola A, Shao R, Kawaguchi Y, Ito A, Nixon A, Yoshida M, Wang XF, Yao TP: HDAC6 is a microtubule-associated deacetylase. *Nature* 2002, 417(6887):455-458.

20. Zhang X, Yuan Z, Zhang Y, Yong S, Salas-Burgos A, Koomen J, Olashaw N, Parsons JT, Yang XJ, Dent SR *et al*: HDAC6 modulates cell motility by altering the acetylation level of cortactin. *Mol Cell* 2007, 27(2):197-213.

21. Falkenberg KJ, Johnstone RW: Histone deacetylases and their inhibitors in cancer, neurological diseases and immune disorders. *Nat Rev Drug Discov* 2014, 13(9):673-691.

22. Bartok B, Firestein GS: Fibroblast-like synoviocytes: key effector cells in rheumatoid arthritis. *Immunol Rev* 2010, 233(1):233-255.

23. Lee J, Hong EC, Jeong H, Hwang JW, Kim H, Bae EK, Ahn JK, Choi YL, Han J, Cha HS *et al*: A novel histone deacetylase 6-selective inhibitor suppresses synovial inflammation and joint destruction in a collagen antibody-induced arthritis mouse model. *Int J Rheum Dis* 2015, 18(5):514-523.

24. Komatsu N, Takayanagi H: Inflammation and bone destruction in arthritis: synergistic activity of immune and mesenchymal cells in joints. *Front Immunol* 2012, 3:77.

25. Creppe C, Malinouskaya L, Volvert ML, Gillard M, Close P, Malaise O, Laguesse S, Cornez I, Rahmouni S, Ormenese S *et al*: Elongator controls the migration and differentiation of cortical neurons through acetylation of alpha-tubulin. *Cell*

2009, 136(3):551-564.

26. Deakin NO, Turner CE: Paxillin inhibits HDAC6 to regulate microtubule acetylation, Golgi structure, and polarized migration. *J Cell Biol* 2014, 206(3):395-413.

27. Wang YH, Yan ZQ, Qi YX, Cheng BB, Wang XD, Zhao D, Shen BR, Jiang ZL: Normal shear stress and vascular smooth muscle cells modulate migration of endothelial cells through histone deacetylase 6 activation and tubulin acetylation. *Ann Biomed Eng* 2010, 38(3):729-737.

28. Kaluza D, Kroll J, Gesierich S, Yao TP, Boon RA, Hergenreider E, Tjwa M, Rossig L, Seto E, Augustin HG *et al*: Class IIb HDAC6 regulates endothelial cell migration and angiogenesis by deacetylation of cortactin. *EMBO J* 2011, 30(20):4142-4156.

29. Zhang Y, Zhang M, Dong H, Yong S, Li X, Olashaw N, Kruk PA, Cheng JQ, Bai W, Chen J *et al*: Deacetylation of cortactin by SIRT1 promotes cell migration. *Oncogene* 2009, 28(3):445-460.

30. Palmer G, Gabay C, Imhof BA: Leukocyte migration to rheumatoid joints: Enzymes take over. *Arthritis Rheum* 2006, 54(9):2707-2710.

31. Ahmed S, Riegsecker S, Beamer M, Rahman A, Bellini JV, Bhansali P, Tillekeratne LM: Largazole, a class I histone deacetylase inhibitor, enhances TNF-alpha-induced ICAM-1 and VCAM-1 expression in rheumatoid arthritis synovial

fibroblasts. *Toxicol Appl Pharmacol* 2013, 270(2):87-96.

32. Soo Youn G, Ju SM, Choi SY, Park J: HDAC6 mediates HIV-1 tat-induced proinflammatory responses by regulating MAPK-NF-kappaB/AP-1 pathways in astrocytes. *Glia* 2015.

33. Sakaguchi S, Sakaguchi N, Asano M, Itoh M, Toda M: Immunologic self-tolerance maintained by activated T cells expressing IL-2 receptor alpha-chains (CD25). Breakdown of a single mechanism of self-tolerance causes various autoimmune diseases. *J Immunol* 1995, 155(3):1151-1164.

34. Tai X, Van Laethem F, Pobezinsky L, Guinter T, Sharrow SO, Adams A, Granger L, Kruhlak M, Lindsten T, Thompson CB *et al*: Basis of CTLA-4 function in regulatory and conventional CD4(+) T cells. *Blood* 2012, 119(22):5155-5163.

35. Hori S, Nomura T, Sakaguchi S: Control of regulatory T cell development by the transcription factor Foxp3. *Science* 2003, 299(5609):1057-1061.

36. Beier UH, Wang L, Han R, Akimova T, Liu Y, Hancock WW: Histone deacetylases 6 and 9 and sirtuin-1 control Foxp3+ regulatory T cell function through shared and isoform-specific mechanisms. *Sci Signal* 2012, 5(229):ra45.

37. Meiler E, Nieto-Pelegrin E, Martinez-Quiles N: Cortactin tyrosine phosphorylation promotes its deacetylation and inhibits cell spreading. *PLoS One* 2012, 7(3):e33662.

38. Tilghman RW, Hoover RL: The Src-cortactin pathway is

required for clustering of E-selectin and ICAM-1 in endothelial cells. *FASEB J* 2002, 16(10):1257-1259.

List of abbreviations

ACR	American College of Rheumatology
AIA	Adjuvant-induced arthritis
CAIA	Collagen antibody-induced arthritis
CCK-8	Cell-counting kit 8
CFSE	Carboxyfluorescein succinimidyl ester
CIA	Collagen-induced arthritis
DMSO	Dimethyl sulfoxide
ELISA	Enzyme-linked immunosorbent assay
FBS	Fetal bovine serum
FLS	Fibroblast-like synoviocytes
HAT	Histone acetyltransferase
HC	Healthy control or healthy donor
HDAC	Histone deacetylase
HDACi	Histone deacetylase inhibitor
Hsp	Heat shock protein
IFN	Interferon
IL	Interleukin
iTreg	Induced regulatory T cells
LPS	Lipopolysaccharide
Luminex assay	Magnetic Luminex Screening Assay multiplex kit
M808	CKD-M808

MAPK	Mitogen-activated protein kinase
MMP	Metalloproteinase
MFI	Mean fluorescence intensity
NC	Nitrocellulose
NES	Nuclear export signal
NLS	Nuclear localization signal
P/S	Penicillin/streptomycin
Pan-HDACi	Pan-HDAC inhibitor
PBMC	Peripheral blood mononuclear cell
PBS	Phosphate buffered saline
RA	Rheumatoid arthritis
RPMI	RPMI 1640
Secondary antibody	Horseradish peroxidase-conjugated anti-mouse or anti-rabbit immunoglobulin
Sirt	Sirtuin
TBST	Tris-buffered saline containing 0.05% Tween 20
Teff	Effector T cells
TNF	Tumor necrosis factor
Treg	Regulatory T cells
Vitamin D_3	1,25-dihydroxyvitamin D_3

국문 초록

새로운 히스톤 탈아세틸화효소 6 억제제인 CKD-M808이 류마티스 관절염 환자의 활막세포와 조절 T 세포에 미치는 영향

서울대학교 융합과학기술대학원
분자의학 및 바이오제약학과
손세희

배경: 류마티스 관절염은 만성 자가면역성 염증 질환으로, 활막세포의 증식과 백혈구의 침윤에 의한 골 파괴가 전형적인 특징이다. 히스톤 탈아세틸화효소 억제제는 자가면역질환을 포함한 많은 질병에서 치료제로 알려져 왔다. 그러나 범 히스톤 탈아세틸화효소 억제제는 최근 임상 시험에서 독성이 보고되었으며, 그에 따라 히스톤 탈아세틸화효소의 선택적 억제의 필요성이 대두되었다. 히스톤 탈아세틸화효소 6는 주로 히스톤이 아닌 단백질을 대상으로 작용하는 효소이다.

목적: 본 연구에서는 류마티스 관절염 환자의 활막세포와 말초 혈액 단핵구 세포, 조절 T 세포, 그리고 동물모델에서 새로운 선택적 히스톤 탈아세틸화효소 6 억제제인 CKD-M808 (M808)의 항 염증 효과를 연구하였다.

실험방법: 세포 생존능은 Cell-counting kit 8에 의해 분석되었다. 류마티스 관절염 환자의 활막세포는 히스톤 탈아세틸화효소 6 억제제인 tubastatin A 또는 M808 처리 후에 IL-1β로 자극되었다. 활막세포 상층액의 MMP-1, MMP-3, IL-6, CCL2, CXCL8, CXCL10의 농도는 Luminex assay와 효소결합면역흡착측정법으로 측정하였다. 활막세포에서의 히스톤 탈아세틸화효소 6, 아세틸화 튜불린, 튜불린, 아세틸화 cortactin, cortactin, GAPDH의 단백질 발현은 웨스턴 블롯으로 평가하였다. 또한, 활막세포에서 상처 치유 분석과 세포 부착 분석이 수행되었다. 류마티스 관절염 환자의 말초 혈액 단핵구 세포는 tubastatin A 또는 M808으로 처리 후에 LPS로 자극되었다. 말초 혈액 단핵구 세포 상층액의 TNF-α, IL-1β, IL-6, IL-10의 농도는 Luminex assay와 효소결합면역흡착측정법으로 측정하였다. CD4+CD25- T 세포는 류마티스 관절염 환자의 말초 혈액 단핵구 세포에서 분리되었다. 분리된 세포들은 조절 T 세포로 분화 유도되었고, 조절 T 세포의 표지자 발현 정도는 유세포 분석으로 측정되었다. 건강인 기증자로부터 얻어진 CD4+CD25- T 세포는 CFSE로 염색한 후 류마티스 관절염 환자의 조절 T 세포와 함께 공배양되었다. 마우스 비장세포로부터 얻어진 CD4+CD25+ T 세포 (조절 T 세포) 는 eFluor®670로 염색한 동일 유래의 CD4+CD25- T 세포와 함께 배양되었다. CD4+CD25- T 세포의 증식은 유세포 분석으로 측정하였다. Lewis rat에서 adjuvant 유도성 관절염 모델을 만든 후, 몸무게와 관절염의 임상 점수를 측정하여 평가하였다.

실험결과: M808은 세포독성 없이 류마티스 관절염 환자의 활막세포에서 MMP-1, MMP-3, IL-6, CCL2, CXCL8, CXCL10과 같은 염증성

인자들의 농도를 감소시켰다. M808은 류마티스 관절염 환자의 활막세포에서 튜불린과 cortactin의 아세틸화를 증가시켰고, ICAM-1과 VCAM-1의 발현을 저해시켰다. 류마티스 관절염 환자의 활막세포의 이동과, U937 세포와 Jurkat 세포의 활막세포에의 부착은 M808의 처리로 인해 감소되었다. M808은 류마티스 관절염 환자의 말초 혈액 단핵구 세포에서 세포독성을 보이지 않으면서 TNF-α는 감소시키고 IL-10을 증가시켰지만, IL-1β와 IL-6에서는 큰 영향을 보이지 않았다. M808 2μM 처리 군에서 사람 T 세포에서 조절 T 세포로의 분화율이 감소되었음에도 불구하고, M808 존재 하에서 사람 조절 T 세포의 억제 능력은 상당히 향상되었다. 또한 M808은 마우스 CD4+CD25- T 세포의 증식을 억제할 뿐만 아니라 마우스 조절 T 세포의 억제 능력도 향상시켰다. M808은 AIA 래트 모델에서 몸무게를 증가시키고 임상 점수를 낮추는 효과를 보였다.

결론: 새로운 히스톤 탈아세틸화효소 6 억제제인 M808은 류마티스 관절염 환자로부터 유래된 세포들의 염증성 인자들의 발현을 줄이고, 세포 이동과 부착을 감소시키고, 조절 T 세포의 기능을 향상시켰다. 또한 동물모델에서도 관절염 임상 점수를 낮추는 등의 치료 효능을 보였다. 따라서 M808은 류마티스 관절염의 잠재적인 치료제제가 될 수 있다고 사료되었다.

주요어: 히스톤 탈아세틸화 효소 6, 히스톤 탈아세틸화효소 억제제, 류마티스 관절염, 염증, 활막세포, 조절 T 세포, 세포 이동

학번: 2015-26078